

# Reconstruction of 3D Neurovascular Models

Jingyi Zuo  
Computer Science  
UCLA  
jzuo1998@gmail.com

Xuan Peng  
Computer Science  
UCLA  
syaziran@gmail.com

Junting Luo  
Computer Science  
UCLA  
misterbig030@gmail.com

## I. INTRODUCTION

Faced with various diseases that have close connection with different organs and tissues of humans, people always try to get a clearer view of the internal structure of the human body. There are many difficulties in analyzing the internal tissues and structures of the human body and compared to many other components in our body, brain vessels are more complex. While there are other technologies that can provide us a 3D reconstructed model of brain vessels, limited to the time and efficiency, X-Ray angiography is most widely used during surgery.

3D reconstruction is a popular and important research topic in computational imaging. People already got many outcomes in this field. Our approach, different from traditional computerized tomography (CT) scan using multiple views from different angles, tries to reconstruct 3D model from only two views. Not as 3D reconstruction from multi-views which has more information and perspectives for calculating the right 3D coordinates, 3D reconstruction from single or biplane view always have more difficulties. Current researches have already achieved many outcomes, but some problems, like difficulty in making point correspondence and dealing with miscellaneous points still exist in biplane view methods and require future optimization.

## II. METHODOLOGY

Various of distinct reconstruction strategies had been proposed in the area of 3D blood vessel reconstruction while most of them assent to the same geometric assumption. In this section, theoretical basis and mathematical models that generally applies to reconstruction problem will be discussed and our implementation closely follows this guideline.

### A. Single Plane Model

Single perspective angiography is one of the most widely used medical imaging techniques and diagnosis basis in clinic. High-energy electromagnetic radiation penetrate patient's body and an x-ray image is obtained in different shades of black and white due to the density and absorption differences.

In Fig.1, monoplane projection geometry and mathematical model are presented, regarding the X-Ray source as the world space origin. In this model, a point in world space with coordinate  $X_i = (x_i, y_i, z_i)^T$  is projected to a two-dimension point  $u_i = (\mu_i, \nu_i)^T$  on the image plane. This transformation

can be generalized as the following mapping between three-dimension points and two-dimension points [6]

$$(x_i, y_i, z_i)^T \mapsto (SID \cdot x_i / z_i + u_c, SID \cdot y_i / z_i + v_c)^T \quad (1)$$

where  $SID$  is the source to image intensifier distance and  $(u_c, v_c)$  is the projected coordinate of iso-center on image plane.

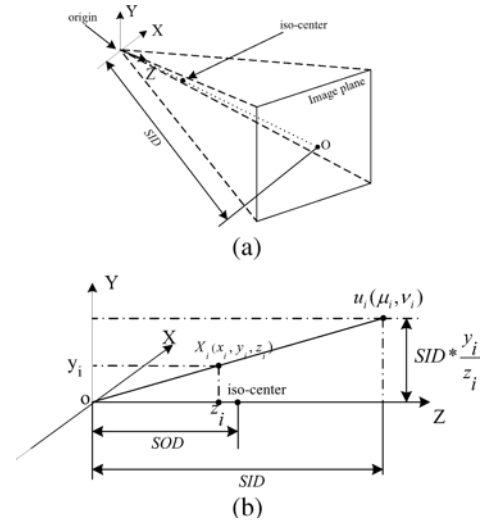


Fig. 1: Imaging model of a monoplane angiography system. (a) Projection geometry. (b) Mathematical Model [6].

Introducing homogeneous coordinates into our projection system, the mapping function [6] can be transformed to

$$\begin{pmatrix} x_i \\ y_i \\ z_i \\ 1 \end{pmatrix} \mapsto \begin{pmatrix} \frac{SID}{\alpha_u} & s \cdot \frac{SID}{\alpha_v} & u_c & 0 \\ 0 & \frac{SID}{\alpha_v} & v_c & 0 \\ 0 & 0 & 1 & 0 \end{pmatrix} \begin{pmatrix} x_i \\ y_i \\ z_i \\ 1 \end{pmatrix} = P X_i \quad (2)$$

in which  $\alpha_u$  and  $\alpha_v$  are the image width and height in pixels, and  $s$  is referred to as the skew parameter. Among all the parameters above, some are introduced from intrinsic settings of C-arm which is known from DICOM (Digital Imaging and Communications in Medicine) image files. If not provided, such intrinsic parameters can be determined by semi-automatic camera calibration. Splitting such parameters from the projection matrix, a concise form of equation is obtained

$$X_i \mapsto K[I|0]X_i = P X_i \quad (3)$$

where  $I$  is  $3 \times 3$  identity matrix and  $K$  is a  $3 \times 3$  matrix

$$K = \begin{pmatrix} \frac{SID}{\alpha_u} & s \cdot \frac{SID}{\alpha_v} & u_c \\ 0 & \frac{SID}{\alpha_v} & v_c \\ 0 & 0 & 1 \end{pmatrix} \quad (4)$$

The projection matrix in (3) has been rewrote to a multiplication of two matrices  $K$  and  $[I|0]$ , representing camera's intrinsic and extrinsic parameters correspondingly. Camera's intrinsic information such as SID and skew parameter is usually determined by camera setting and projection model, while extrinsic parameters illustrate camera's spatial rotation and translation.

### B. Biplane Model

Biplane reconstruction involves a transformation of camera position which changes the projection matrix and the mathematical model in previous section no longer works. Therefore, two-view angiographic projection set up two coordinates systems as shown in Fig. 2 and the extrinsic parameters quantify the relationship between camera positions (X-Ray sources).

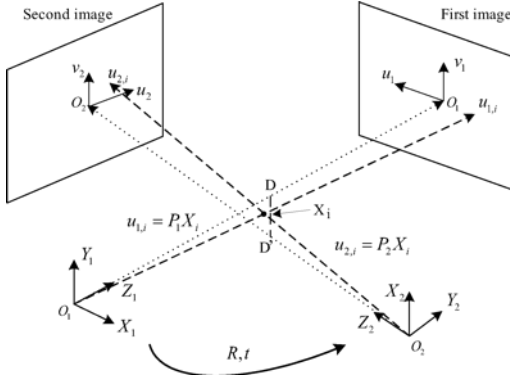


Fig. 2: Geometric relationship between two angiographic views.  $O_1$  and  $O_2$  represent the X-Ray source positions [6].

Apply (3) to the model in Fig. 2 and a system of functions can be formulated as

$$\begin{aligned} u_{1,i} &= K[I|0]X_i \\ u_{2,i} &= K[R|t]X_i \end{aligned} \quad (5)$$

where  $u_{1,i}$  and  $u_{2,i}$  are projected coordinates of a same point  $X_i$  on each image plane,  $R$  is  $3 \times 3$  rotation matrix, and  $t$  is a translation vector [6]. A set of three equations is derived from cross product  $u_1 \times (P_1 X) = 0$  as

$$\begin{aligned} \mu_1(p_1^{3T} X) - (p_1^{1T} X) &= 0 \\ \nu_1(p_1^{3T} X) - (p_1^{2T} X) &= 0 \\ \mu_1(p_1^{2T} X) - \nu_1(p_1^{1T} X) &= 0 \end{aligned} \quad (6)$$

where  $p_i^{jT}$  is the  $j$ th row of the projection matrix  $P_i$  [6]. Similarly, three more equations can be derived from another cross product  $u_2 \times (P_2 X) = 0$ . As shown above in (6), only two

of equations are linearly independent; therefore, the whole equation system can be eliminated down to matrix form [6]

$$\begin{pmatrix} \mu_1 p_1^{3T} - p_1^{1T} \\ \nu_1 p_1^{3T} - p_1^{2T} \\ \mu_2 p_2^{3T} - p_2^{1T} \\ \nu_2 p_2^{3T} - p_2^{2T} \end{pmatrix} X = 0 \quad (7)$$

The relationship between a space point and its projection on image planes in (7) can successfully reconstruct the three-dimension coordinates if correspondences between interest points  $(u_{1,i}, u_{2,i})$  are known.

### C. Epipolar Constraint

Prior to actual reconstruction, feature detection [5] and feature matching is necessary to obtain effective and accurate point correspondences. Many precedent researches on feature detection focused on salient points and the loss of detail will dramatically weaken our reconstruction result. Thus, instead of using feature detection algorithms, we extract a tiny patch for each point and match it with other points [1]. Feature matching with vessel centerline [2] effectively generate correspondences among points on image planes. In conventional feature matching process, nearest neighbour search in the feature space, such as brute-force search and Fast Library for Approximate Nearest Neighbors (FLANN) are widely used. However, due to the complication of input images, epipolar geometry is introduced to optimize our matching process by narrowing down the feature space.

Epipolar constraint is the restriction relationship between the epipolar plane and the epipolar line, assuming corresponding features are projections from the same three-dimension point [7]. As shown in Fig. 3,  $u_{2,o}$  is coplanar with  $O_1$ ,  $O_2$ , and  $u_{1,i}$ . According to this spatial relationship, a planar constraint can be applied

$$(\overrightarrow{O_1 u_{1,i}} \times \overrightarrow{O_1 O_2}) \cdot \overrightarrow{O_2 u_{2,i}} = 0 \quad (8)$$

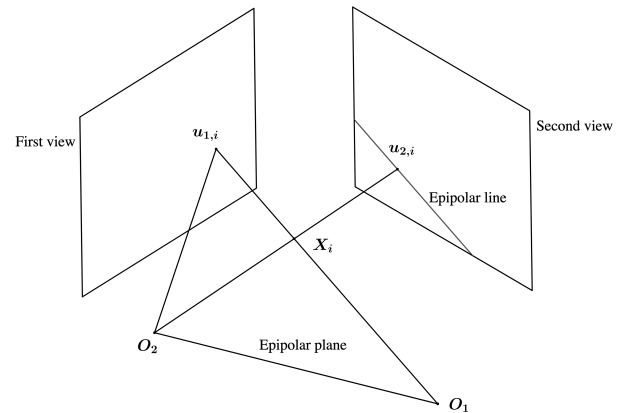


Fig. 3: Epipolar constraints for two angiograms.

A unique epipolar line therefore is determined as the intersection of plane  $O_1 O_2 u_{1,i}$  and the second image plane. Along this epipolar line, we can loop over all points and find the best

matched patch to pair up with  $u_{1,i}$  as a correspondence. Many metrics evaluating the accuracy of a match exist; among them, Sum of Squared Differences (SSD) and Normalized Cross Correlation (NCC) are most commonly used.

### III. EVALUATION

For evaluating the result of our implementation and summing up valuable conclusions, we set different criteria and used different kinds of test cases to check the differences among the outputs in different situations.

#### A. Criteria

We evaluate our implementation through comparing the output models to the original 3D models that we extract our 2D image inputs from two criteria. The first one is the accuracy of locating the 3D points and the other one is the effect of miscellaneous points on the results. The accuracy of locating the 3D points affects the overall effect of the reconstruction since determine the 3D coordinate of each points on the model is the fundamental part of the 3D model reconstruction. The rate of resulting miscellaneous points is inversely proportional to the visual effect of the reconstructed 3D models.

These two criteria reflect the main problems that in current biplane view 3D reconstruction methods. While doing reconstruction from multi-view, we usually have more clues to extract the accurate 3D points coordinates. From biplane view, we are faced too much more difficulties in solving this problem, especially when we try to reconstruct complex 3D models that have a lot of interlaced nerves and vessels. In this case, the low accuracy of calculated coordinates and the increasing miscellaneous points will eventually affect the results of our reconstruction.

#### B. Cases

Considering the effects those complex cases may bring when we reconstruct 3D neurovascular models, we evaluate our project in two different kinds of cases. One case is we use a simple 3D vessel model to extract two 2D images as our inputs to do the reconstruction. The other case is a most complex 3D neurovascular model that provided in the <http://cng.gmu.edu/> website. .

Through testing on simple models, we try to evaluate if our implementation can work on reconstructing some basic 3D vascular models from biplane view at first. Evaluating on the complex models after that reflects the final propose of our project. When we apply our implementation on a most complex model, we can see if more problems occur and what criteria are matched worse. Comparing the results of the two different kinds of test cases, we can get more clues on how well 3D reconstruction from biplane view can make and what problems needed to be optimized in this study field.

### IV. RESULTS

#### A. Results of Reconstructing Simple Vascular Model

When we applied our implementation on two 2D images extracted from a simple 3D vascular Model, the result was

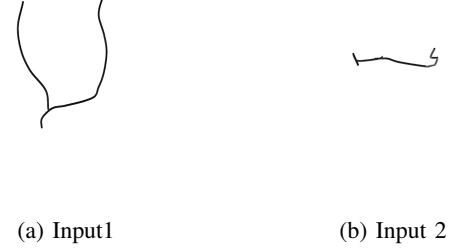


Fig. 4: 2D images inputs

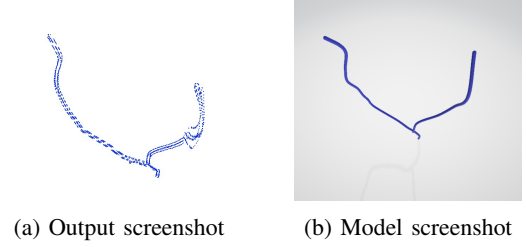


Fig. 5: Output vs Model

fairly consistent with the original 3D model from all sides. Figure 4 shows out two 2D image inputs. We extracted these two images by taking screenshots of the original 3D model from different angles. The first image was taken from -1 degree and the second one was taken from 89 degree along x axis. These data are used as angle parameters in our implementation and are important for reconstruction. Figure 5 shows screenshots of the result and the original model from an angle different from the input images. By contrast, we can see that the accuracy of calculating 3D points is pretty good while the rate of miscellaneous points is low. Therefore, our method can successfully reconstruct simple 3D neurovascular models from biplane view.

#### B. Results of Reconstructing Complex Neurovascular Model

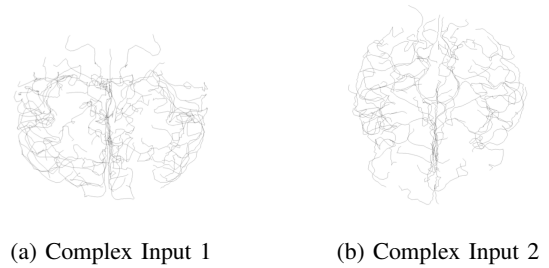


Fig. 6: Complex Image Inputs

When we apply our method on the most complex neurovascular model, the result gets complicated. Since our goal is to reconstruct 3D models from biplane view, our implementation based on existing algorithms don't provide very ideal outputs when we used inputs extracted from complex models. As Figure 6 shows, the input images contain a lot of interlaced



Fig. 7: Screenshot of Output Complex 3D Model.

blood vessels and points covering each other. It is very difficult to accurately determine the three-dimensional coordinates of these points in such complex cases. Figure 7 is a screenshot of our resulting 3D model. As it shows, running our program with these two 2D images, points that hard to tell from input angles couldn't be relocated into 3D coordinate accurately and we got a reconstructed 3D model with many miscellaneous points. Compared to the previous simple case, we saw some limitations of 3D neurovascular model reconstruction from biplane view. During the process of studying the biplane algorithms for this project, we searched and discussed a lot on it.

## V. DISCUSSION

Throughout the project, we did a lot of research on existing biplane 3D reconstruction algorithms and 3D reconstruction by some other methods. We tried various of these methods for improving the effect of reconstructing 3D points from biplane views, and eventually decided our method as shown in previous sections. However, this method is not perfect and has downsides that are hard to resolve.

One problem of such technique is that it's hard to find the 3D corresponding point from two pixels of different images. It's challenging to find correspondence between two pixels from the input images and decide whether they come from the same 3D point. As a result, more than one hypothetical 3D point predictions are created because of the uncertainty.

Another disadvantage for reconstructing from biplane views is that only two images are used for reconstructing the model. Although by comparing and calculating the 2D points from each image by their epipolar lines we can determine their corresponding 3D points in world space model, there are still a lot of spots in space which cannot be determined or captured uniquely from just two angles of projections. There could easily be points in space where they are hidden behind other points from both perspectives so that their existence in the 3D model cannot be proved from just two input images. Therefore, noises are inevitable in our results. [4]

One of the reason that our result is not perfect is that we did not use DICOM files as our input. Instead, we use 2D projections captured by the model as input. Therefore we don't have the intrinsic parameters provided by the camera automatically. To derive these settings, we have to manually calibrate such parameters semi-automatically [8]. The result of

such manual settings therefore induces errors from the input files themselves.

We also tried connecting our reconstructed 3D points manually by grouping the points by their relative distance and drawing lines to represent real vessels instead of merely displaying points in space. We wrote an algorithm to search for the closest point for each 3D point and connect each cluster, but the result is unstable and sometimes incorrect because of miscellaneous points. It's also much more complicated than real vessels where the reconstructed 3D points are much denser than our algorithm's minimum threshold distance, when it would draw a ball of lines over a particular spot. So we realize that it's more natural to just leave the reconstructed points as they are.

Another alternative method that we considered is filtered back projection algorithm, which is a stabilized and discretized version of inverse Radon transform. This method tries to invert the Radon transform of the model and recover the initial model. It takes as input a pair of projections and the angular spacing between them, and a radon kernel with its frequency response. This method produces better resolution, but it induces much greater noise in our result because the filter tends to amplify the high-frequency content. [3]

## VI. FUTURE WORK

For future study, there could still be some post-processing methods that can be applied to mitigate noises in the result.

For example, we can use bundle adjustment to minimize errors of our predictions and use algorithms such as Levenberg-Marquardt Algorithm to implement non-linear least squares optimization. We can create an objective function by taking the sum of squares of the difference between the 2D coordinates of the projection of our predicted 3D points on our input view plane and our actual 2D point input. Then we can use Gauss-Newton Method and linearize the objective function, which can then be minimized by taking partial derivatives to get our initial solution. If the solution does not converge, then we can use Levenberg-Marquardt Algorithm to combine the characteristic of Gauss-Newton Method and gradient descent. These methods could potentially reduce the number of miscellaneous points in our model.

Another technique that can be introduced to the system is Frangi filter, which can enhance the vessel structure by computing the likelihood of the blood vessel using eigenvectors and Hessian matrix. We can also try to re-project our result model on our input projection plane and filter out points that don't overlap with our original 2D points. This process corrects any errors and mistakes made during reconstruction. As stated in previous sections, our result is not perfect and should be post-processed with more proper methods.

## VII. CONCLUSION

In conclusion, this project aims to reconstruct the 3D model of blood vessels by taking biplane views of the model as input. It utilizes stereo image reconstruction algorithms to match each 2D input pixel to its corresponding 3D position.

Through this project, we have a certain understanding of 3D reconstruction. We've learned a lot about the current approaches to 3D reconstruction of neurovascular model and some problems that exist with this technology and need to be optimized. By evaluating our results on both simple and complex cases, we are able to reconstruct the 3D model with great similarity to the actual model for simple 3D model cases, but have more errors when finding all the 3D points coordinate for some complex models. Our results can still be improved by applying optimization algorithms and enhancing the vessel structure. In order to achieve more accurate 3D neurovascular reconstruction from biplane or by some other methods, people still need to improve existing technologies and optimize the algorithm. Our performance is promising and can provide some necessary assistance to study neurovascular structure.

#### REFERENCES

- [1] Y. Furukawa and C. Hernández. *Multi-View Stereo: A Tutorial*. 2015.
- [2] H. Greenspan, M. Laifenfeld, S. Einav, and O. Barnea. Evaluation of center-line extraction algorithms in quantitative coronary angiography. *IEEE Transactions on Medical Imaging*, 20(9):928–941, 2001.
- [3] I. K. Hong, S. T. Chung, H. K. Kim, Y. B. Kim, Y. D. Son, and Z. H. Cho. Ultra fast symmetry and simd-based projection-backprojection (ssp) algorithm for 3-d pet image reconstruction. *IEEE Transactions on Medical Imaging*, 26(6):789–803, 2007.
- [4] H. Kim, Seung-jun Yang, and Kwanghoon Sohn. 3d reconstruction of stereo images for interaction between real and virtual worlds. In *The Second IEEE and ACM International Symposium on Mixed and Augmented Reality, 2003. Proceedings.*, pages 169–176, 2003.
- [5] Yan Ke and R. Sukthankar. Pca-sift: a more distinctive representation for local image descriptors. In *Proceedings of the 2004 IEEE Computer Society Conference on Computer Vision and Pattern Recognition, 2004. CVPR 2004.*, volume 2, pages II–II, 2004.
- [6] J. Yang, Y. Wang, Y. Liu, S. Tang, and W. Chen. Novel approach for 3-d reconstruction of coronary arteries from two uncalibrated angiographic images. *IEEE Transactions on Image Processing*, 18(7):1563–1572, 2009.
- [7] Z. Zhang. Determining the epipolar geometry and its uncertainty: A review. *International journal of computer vision*, 27(2):161–195, 1998.
- [8] Z. Zhang. A flexible new technique for camera calibration. *IEEE Transactions on Pattern Analysis and Machine Intelligence*, 22(11):1330–1334, 2000.